Magazine of Civil Engineering. 2020. 95(3). Pp. 119–130

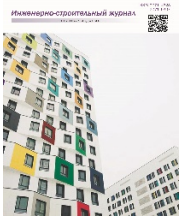

Magazine of Civil Engineering

ISSN 2071-0305

journal homepage: http://engstroy.spbstu.ru/

DOI: 10.18720/MCE.95.11

Deformed state of the bases buildings and structures from weak viscoelastic soils

***T.V. Maltseva*[a]*, E.R. Trefilina*[b], *T.V. Saltanova*[b]**

[a] *Industrial University of Tyumen, Tyumen, Russia*

[b] *Tyumen State University, Tyumen, Russia*

** E-mail: maltv@utmn.ru*

Keywords: soft soils, water-saturated base, stresses and deformation, viscoelasticity of the soil, modeling of bearing capacity

Abstract. The article discusses the grounds of buildings and structures from weak viscoelastic soils, the features of the theoretical justification for their deformations. The need for this study is due to the discrepancy between the theory of filtration consolidation and field and laboratory experiments. Within the framework of the proposed model, the constructions of solutions to the problems of loading the ground surface with typical loads that describe the stress-strain state of each phase of a two-phase medium (soil skeleton + pore water) with account of the residual pore pressure. The deviation of the calculated residual pore pressures from the experimental data is not more than 5 % (laboratory experiment), 7 % (full-scale experiment). The calculation method presented in the article allows predicting the deformation of the foundations of structures from weak water-saturated soils.

1. Introduction

In connection with the increase in housing and industrial construction, the problem of erecting and operating industrial and civil structures on soft water-saturated soils, as a result of the development of new territories, is becoming especially relevant. Despite the successful construction and operation of buildings and structures on soft water-saturated soils in general, in practice, one has to deal with deformations of such structures. The analysis shows that the cause of deformations which result in emergency conditions of structures is the insufficient consideration of strength properties, permeability, creep of soils [1]. For soft water-saturated soils (more than 80 % of the pores of the soil are filled with water) there are also special patterns of their deformability [2].

Speakers at international conferences devoted to these problems put forward a number of causes of deformations of structures located on the soils under consideration. They highlight three main features for soft soils. The first is the high compressibility of soils, the second is low strength, and the third is the long duration of settlement of structures [3]. In most cases, soft water-saturated soils cannot be used as the foundation of buildings and structures without their reinforcement through the use of geosynthetics, the construction of sand contour-reinforced piles, sand cushions, etc. [4–13].

Modern calculations of foundations and bases on soft water-saturated soils are carried out with account of the specifics of their properties, creep of the soil skeleton [14], compressibility of pore water [15–17] and filtration consolidation. Research into the determination of the stress-strain state of soil bases establishes the limits of applicability of methods for their calculation.

In particular, the analysis of the models of the theory of filtration consolidation based on a system of parabolic equations [18] shows that the residual pore pressures necessarily turn to zero and the two-phase system becomes a single-phase one (curve 1, Fig. 1). However, starting from some time T_{st}, field and laboratory tests [19, 20] show the presence of excessive pore pressure in a stabilized state. Filtration

Maltseva, T.V., Trefilina, E.R., Saltanova, T.V. Deformed state of the bases buildings and structures from weak viscoelastic soils. Magazine of Civil Engineering. 2020. 95(3). Pp. 119–130. DOI: 10.18720/MCE.95.11

consolidation models are no longer applicable to the description of the stress-strain state of a two-phase (water-saturated) base.

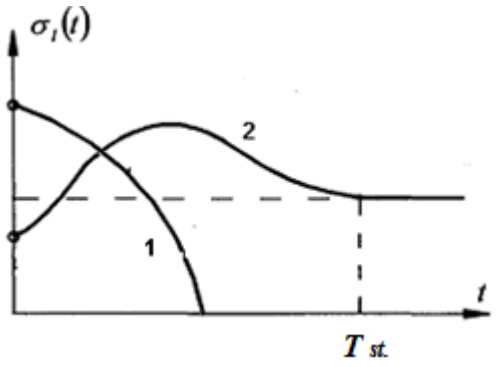

Figure 1. Change in pore pressure over time.

The article discusses a scientific direction based on a system of elliptic equations, describes residual pore pressures [18]. In accordance with the experiment, starting from a depth of 2 m from the ground surface, the qualitative character of the graph of the change in pore pressure over time has the form of curve 2 in Fig. 1. A nonmonotonic change in pore pressure over time corresponds to the consolidation process; a nonzero pore pressure corresponds to a stable state of the system. Soils with low permeability less than 5 10^{-3} m/day.

According to this model, the soil is a continuous two-phase medium. The model is phenomenological, its parameters are found from experiments and it doesn't consider the mechanism of the interaction of phases based on their molecular nature.

The object of the study is a water-saturated soil base, the behavior of which under load is described from the standpoint of the mechanics of a deformable solid with account of the influence of pore water on it ("soil skeleton + pore water" two-phase system). The subject of the study is the effect of residual pore pressure on the deformed state of a water-saturated soil base.

The purpose of the study is to solve the problem of mathematical modeling of the deformed state of the soil base, taking into account the residual pore pressure at the end of the consolidation process. Within the framework of the model under consideration, the construction of solutions to the problems of loading the day surface with typical loads that describe the stress-strain state of each of the phases of a two-phase medium is carried out.

The kinematic model considered in the article describes the stress-strain state of a water-saturated soil base under load (its one-dimensional version is described in the monograph [21]) and is based on two assumptions:

1. The relative deformation of pore water ε_l (l-pore water) is proportional to the difference in pore pressure σ_1, per length unit, i.e., the relative movement of particles of pore water is caused by pressure drop (-) $\varepsilon_l = \frac{h}{E_l}\frac{d\sigma_l}{dz}$.

Relative deformation ε_l describes a local change in pore volume $dn = \varepsilon_l\, dz \cdot A$, where A is the cross-sectional area of the sample.

2. The relative deformation of the particles of pore water and the skeleton of the soil ε_s (s is the skeleton of the soil) are proportional and opposite in sign: $\varepsilon_s = -\aleph\varepsilon_l$.

The parameters $E_l, \aleph$ are found from experiments to test large two-phase samples.

Let us consider the stress state of a water-saturated soil base as a two-phase half-space loaded with a strip load in a cylindrical coordinate system r, θ, z (a fundamental problem of the Flaman type). Statement of the boundary value problem. The normal stresses are decomposed into the sum of the stresses in the solid and liquid phases, the shear stresses in the pore fluid are set equal to zero:

– equations of equilibrium $\frac{\partial(\sigma_{sr} - \sigma_{lr})}{\partial r} + \frac{\partial \tau_{r\theta}}{\partial \theta} + \frac{(\sigma_{sr} - \sigma_{lr}) - (\sigma_{s\theta} - \sigma_{l\theta})}{r} = 0$,

$$\frac{\partial \tau_{r\theta}}{\partial r}+\frac{1}{r}\frac{\partial(\sigma_{s\theta}-\sigma_{l\theta})}{\partial \theta}+\frac{2\tau_{r\theta}}{r}=0;$$

– physical equations $\sigma_{sr}=\frac{E_s}{1-\nu^2}\left(\varepsilon_{sr}+\nu\varepsilon_{s\theta}\right),\quad \sigma_{s\theta}=\frac{E_s}{1-\nu^2}\left(\varepsilon_{s\theta}+\nu\varepsilon_{sr}\right),$

$$\frac{\partial \sigma_{lr}}{\partial r}=\frac{E_l}{h}\varepsilon_{lr},\quad \frac{\partial \sigma_{l\theta}}{\partial \theta}=\frac{E_l}{h}\varepsilon_{l\theta};$$

– geometrical equations $\varepsilon_{s\,r}=\frac{\partial u_{sr}}{\partial r}$, $\varepsilon_{s\,\theta}=\frac{u_{sr}}{r}+\frac{\partial u_{s\theta}}{r\partial \theta}$,

$$\varepsilon_{l\,r}=\frac{\partial u_{lr}}{\partial r},\ \varepsilon_{l\,\theta}=\frac{u_{lr}}{r}+\frac{\partial u_{l\theta}}{r\partial \theta},$$

$$\gamma_{s\,r\theta}=\frac{\partial u_{sr}}{r\partial \theta}+\frac{\partial u_{s\theta}}{\partial r}-\frac{u_{s\theta}}{r};$$

– kinematic equations $\varepsilon_{sr}=-\aleph\,\varepsilon_{lr}$, $\varepsilon_{s\theta}=-\aleph\,\varepsilon_{l\theta}$.

Boundary conditions:

$$\theta=\pm\frac{\pi}{2}\qquad (\sigma_{s\theta}-\sigma_{l\theta})=0,\ \tau_{r\theta}=0,\quad u_{sr}\Big|_{\substack{\theta=0\\ r=L}}=0;\qquad \sigma_{lr}\big|_{r=\rho}=0.$$

We consider the *Boussinesq* problem about the action of a concentrated force F on an elastic half-space in the spherical coordinates R,θ,φ and generalize its fundamental solution to a two-phase half-space.

The statement of a Boussinesq type boundary value problem:

$$\frac{\partial(\sigma_{sR}-\sigma_{lR})}{\partial R}+\frac{1}{R\sin\theta}\frac{1}{R}\frac{\partial \tau_{\phi R}}{\partial \phi}+\frac{1}{R}\frac{\partial \tau_{R\theta}}{\partial \theta}+$$
$$+\frac{2(\sigma_{sR}-\sigma_{lR})-(\sigma_{s\phi}-\sigma_{l\phi})-(\sigma_{s\theta}-\sigma_{l\theta})+\tau_{R\theta}ctg\theta}{R}=0$$

$$\frac{\partial \tau_{R\phi}}{\partial R}+\frac{1}{R\sin\theta}\frac{1}{R}\frac{\partial(\sigma_{s\phi}-\sigma_{l\phi})}{\partial \phi}+\frac{1}{R}\frac{\partial \tau_{\phi\theta}}{\partial \theta}+\frac{3\tau_{R\phi}+2\tau_{\phi\theta}ctg\theta}{R}=0,$$

$$\frac{\partial \tau_{R\theta}}{\partial R}+\frac{1}{R\sin\theta}\frac{1}{R}\frac{\partial \tau_{\theta\phi}}{\partial \phi}+\frac{1}{R}\frac{\partial(\sigma_{s\theta}-\sigma_{l\theta})}{\partial \theta}+\frac{(\sigma_{s\theta}-\sigma_{l\theta}-(\sigma_{s\phi}-\sigma_{l\phi}))ctg\theta+3\tau_{R\theta}}{R}=0,$$

$$\nabla^2(\sigma_{sR}-\sigma_{lR}+(\sigma_{s\theta}-\sigma_{l\theta})+(\sigma_{s\phi}-\sigma_{l\phi}))=0,$$

$$(\sigma_{s\theta}-\sigma_{l\theta})=-(\sigma_{s\phi}-\sigma_{l\phi}),\ \tau_{\theta\phi}=0,\ \tau_{R\theta}=0.$$

In order to set the boundary conditions, we select two hemispheres: S_1 of a small radius (ρ) and S_2 of a large radius (L). We replace the concentrated force F with the equivalent load distributed over the surface $S_1:\sigma_{sR}\big|_{S_1}=-\sigma 0$, displacements u_{sR} on the surface of the sphere S_2 are taken equal to zero: $u_{sR}\big|_{S_2}=0$. On the daylight surface, stresses in the liquid phase are taken to zero.

2. Methods

We will calculate the stress-strain state of a water-saturated soil base by means of expanding the well-known Flaman solution for an elastic single-phase half-plane:

$$\sigma_r = \frac{-2F\cos\theta}{\pi r}, \quad \sigma_\theta = 0, \quad \tau_{r\theta} = 0.$$

This solution, which uses the hypotheses and equations of the one-dimensional version of the kinematic model, is decomposed into the solutions for each phase separately:

$$\sigma_r = \sigma_{sr} - \sigma_{lr},$$

$$\varepsilon_l = \frac{h}{E_l}\frac{d\sigma_l}{dz}, \ \varepsilon_s = \frac{1-\nu^2}{E_s}\sigma_s,$$

$$\varepsilon_l = \frac{du_l}{dz}, \ \varepsilon_s = \frac{du_s}{dz}, \ \varepsilon_s = -\aleph\,\varepsilon_l.$$

The system of equations is reduced to one differential equation of the first order in the displacements of the solid phase. Its solution has the following form:

$$u_{sr} = \frac{2F\left(1-\nu^2\right)\cos\theta}{\pi E_s}\cdot e^{-a^2 r}\left[\ln\frac{R}{a^2 r} - \int\frac{e^{a^2 r}-1}{r}dr\right],$$

We determine the tangential displacements of the solid phase:

$$u_{s\theta} = \frac{2F\sin\theta}{\pi E_s}\left(\nu\left(1+\nu\right) + \left(1-\nu\left(1+\nu\right)a^2 r\right)\cdot e^{-a^2 r}\left[\ln\frac{R}{a^2 r} - \int\frac{e^{a^2 r}-1}{r}dr\right]\right).$$

Basing on this fundamental solution, we get a solution for a number of problems, which are given below.

The calculation of the elastic two-phase half-space in the stabilized state is carried out by expanding the well-known Boussinesq solution into two phases [18] (similar to the expansion of the Flaman solution):

$$\sigma_{sR} - \sigma_{lR} = -\frac{3F}{2\pi}\cdot\frac{\cos\theta}{R^2}.$$

This equation is the equation of static equilibrium. We supplement it with the equations of the kinematic model for the one-dimensional case and the stabilized state (as in the case of the Flaman solution expansion), reduce the system to a first-order differential equation for the displacements of the solid phase, after integration of which we have the calculation formula for the displacements:

$$u_{sR} = \frac{3F\cos\theta}{2\pi E_s}\cdot\left(e^{-a^2 L}\cdot\int_\rho^L\frac{e^{a^2 R}}{R^2}dR - e^{-a^2 R}\cdot\int_\rho^R\frac{e^{a^2 R}}{R^2}dR\right).$$

In a known manner, one can go from spherical coordinates to cylindrical coordinates and obtain the corresponding formulas for the stresses in the skeleton and pore fluid.

For example, we obtained normal vertical stresses in the problem of a uniformly distributed load:

$$\sigma_{lz} = \frac{2q}{\pi}\cdot a^2\int_{-b}^{b}\frac{z^3}{r^3}\cdot e^{-a^2 r}\left[\ln\frac{r}{\rho} + \int_\rho^r\frac{e^{a^2\xi}-1}{\xi}d\xi\right]d\eta,$$

$$\sigma_{sz} = -\frac{2q}{\pi} \cdot \int_{-b}^{b} \left(\frac{z^3}{r^4} - a^2 \cdot \frac{z^3 e^{-a^2 r}}{r^3} \left[\ln \frac{r}{\rho} + \int_{\rho}^{r} \frac{e^{a^2 \xi} - 1}{\xi} d\xi \right] \right) d\eta,$$

$$\rho \le \xi \le r, \quad r = \sqrt{(x-\eta)^2 + z^2}.$$

The obtained analytical dependences make it possible to construct graphs of changes in stresses and displacements in depth (along the OZ axis) and horizontally. Replacing the integral with a variable upper limit with an approximate expression with an error estimate allowed us to speed up the computational process while maintaining an acceptable accuracy of 3 %.

Solving problems with account of the viscoelastic properties of the soil and changes in the stress-strain state of the soil base in time. One of the stages of the study was the study of changes in pore stress over time. For this study, we turned to the linear hereditary theory of viscoelasticity. In order to switch from the image to the original, we used the broken line method proposed by L.E. Maltsev.

The essence of the broken line method is that the function of four arguments $F^*(x, y, z, p)$ is transferred to the function of one argument $F^*(p)$ by means of replacing spatial coordinates at a fixed point with coordinates $x = x_i, y = y_i, z = z_i \ (i = \overline{1,n})$ with the numbers. A system of fixed spatial points for which it is interesting to obtain (expand) a solution in time in each problem is selected individually. The function known in the images $0 \le p$ is approximated by a function of a special form:

$$\phi^*(p) = \phi(0) \cdot \left(1 - \sum_{i=0}^{n} (c_i - c_{i+1}) \frac{1}{p} e^{-pT_i} \right), \ 0 \le p \le \infty, \ T_0 = 0, c_0 = 0, c_{i+1} = 0$$

The original function $\phi(t)$ is known in advance and looks like a broken line:

$$\phi(t) = \phi(0) \cdot \left(h(t) - \sum_{i=0}^{n} (c_i - c_{i+1})(t - T_i) h(t - T_i) \right).$$

Here $h(t)$ is the Heaviside function, $\phi(0), c_i, T_i$ are the desired parameters of the broken line. The parameter $\phi(0)$ is necessarily dimensional, c_i, T_i are dimensionless**.** The arguments t and p are also dimensionless.

Advantages of writing a function as a broken line:

the possibility of approximation with a given accuracy (the number of links can be increased);

the presence of an elementary image according to Laplace-Carson.

The disadvantages of writing include the following: at the point $t = 0$ the broken line will have a finite derivative**,** and with the function $F(t)$ a derivative may be infinite; the broken line reaching the asymptotic value occurs at the final value *t*.

Let us consider how the pore pressure of a half-plane loaded with a uniformly distributed load changes at the initial stage of time.

In the section, $z = 1/5b$ we fix the coordinate point ($z = 1/5b, x = 0$), for which we show the change in pore stresses in time. In the elastic solution for $\sigma_{lz}(z_3 = 1/5b, x = 0)$, in accordance with the Volterra principle we make a change of notation $a^2 \to [a^2(p)]^*$, and obtain the solution to the viscoelastic problem in the images:

$$\sigma_{lz}^{*}=\frac{2q}{\pi}\cdot(a^2)^{*}\cdot\int_{-b}^{b}\frac{(1/5b)^3}{r^3}\cdot e^{-(a^2)^{*}r}\left[\ln\frac{r}{\rho}+\int_{\rho}^{r}\frac{e^{(a^2)^{*}\xi}-1}{\xi}d\xi\right]d\eta,\ r=\sqrt{\eta^2+(1/5b)^2}\ .$$

In accordance with the broken line method, we present the desired original in the form of a broken line:

$$\overline{\sigma}_{lz}(t)=\sigma(0)\cdot\left(1-\sum_{i=0}^{5}(c_i-c_{i+1})(t-T_i)h(t-T_i)\right),\quad c_0=c_6=T_0=0,$$

in which the parameters $\sigma(0),c_i$ are the desired ones, and T_i are given as for the well-known original $a^2(t)$.

We rewrite this spline in images

$$\overline{\sigma}_{lz}^{*}(p)=\sigma(0)\cdot\left(1-\sum_{i=0}^{5}(c_i-c_{i+1})\frac{1}{p}e^{-pT_i}\right).$$

In order to determine the unknown parameters, we compose a system of linear algebraic equations using the conditions for the broken line to coincide in images with the known right-hand side on the point system $p=P_j$:

$$\overline{\sigma}_{lz}^{*}(p=P_j)=\sigma_{lz}^{*}(p=P_j),\ j=1,\ldots,k\ .$$

The points are selected in a special way, for example, $p_j=\dfrac{\ln T_j-\ln T_{j-1}}{T_j-T_{j-1}},\quad T_0=10^{-5}$.

We repeat similar arguments for other points of the half-space.

3. Results and Discussion

Let us consider the results of calculating normal vertical stresses in the problem of a uniformly distributed load (Fig. 2).

$$\sigma_{lz}=\frac{2q}{\pi}\cdot a^2\int_{-b}^{b}\frac{z^3}{r^3}\cdot e^{-a^2r}\left[\ln\frac{r}{\rho}+\int_{\rho}^{r}\frac{e^{a^2\xi}-1}{\xi}d\xi\right]d\eta,$$

$$\sigma_{sz}=-\frac{2q}{\pi}\cdot\int_{-b}^{b}\left(\frac{z^3}{r^4}-a^2\cdot\frac{z^3e^{-a^2r}}{r^3}\left[\ln\frac{r}{\rho}+\int_{\rho}^{r}\frac{e^{a^2\xi}-1}{\xi}d\xi\right]\right)d\eta,$$

$$\rho\le\xi\le r,\quad r=\sqrt{(x-\eta)^2+z^2}\ .$$

The obtained analytical dependences make it possible to construct graphs of changes in stresses and displacements in depth (along the OZ axis) and horizontally.

Below are the graphs of normal stresses in different sections (Fig. 3).

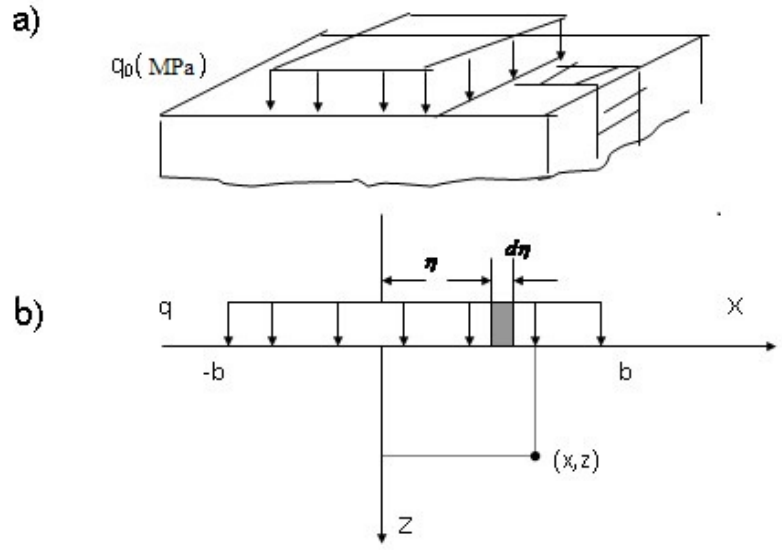

Figure 2. a) Effect of a uniformly distributed load on half-space; b) Transition from distributed load to concentrated force.

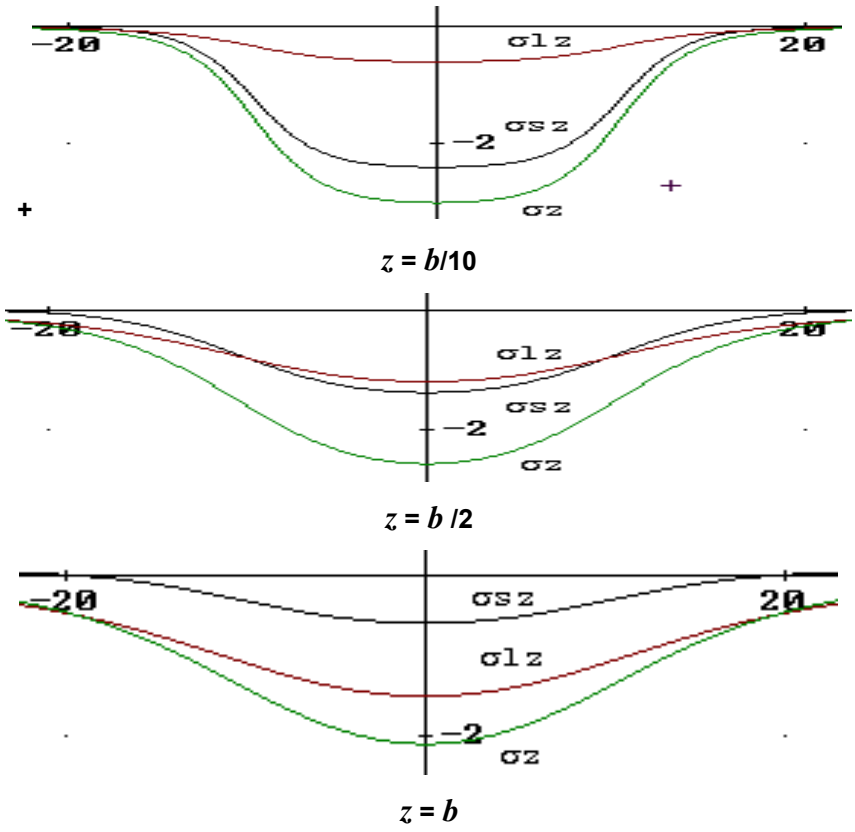

Figure 3. Change in vertical stresses in solid, σ_{sz}, liquid σ_{lz} phases and the total ones σ_z.

In the central part of the loaded area, pore water is more strongly clamped by soil and therefore its bearing capacity is greater than at the periphery. After analyzing the latter graphs of normal stresses, we conclude that at a distance of $z = b$ most of the external load falls on the liquid phase. This once again confirms the carrying capacity of the liquid phase.

In the process of research, we solved the problems of the action of two or more structures on a two-phase base.

Let us consider the problem of determining the stress-strain state of the base from the action of two uniformly distributed loads (Fig. 4). This problem models the mutual influence of two closely standing buildings (flat case). In this case, the stresses and displacements at point M are found through the principle of superposition (summation) of two forces. In order to do this, we first need to place the origin of coordinates at the point of application of force $dF_1 = q_1 d\xi$ and find the coordinates of the point $M(x-\xi_1, z)$. Then we

transfer the coordinates system to the point of application of force $dF_2 = q_2 d\xi$ and determine the new coordinates of the point $M(x-\xi_2, z)$.

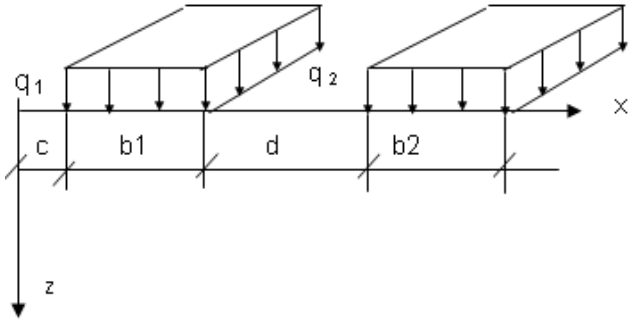

Figure 4. Action of two evenly distributed loads on the base.

Below are the formulas for the stresses:

$$\sigma_{sz} = -\frac{2q_1}{\pi}\int_{c}^{c+b_1} f_1(x,z,\xi)d\xi - \frac{2q_2}{\pi}\int_{c+b_1+d}^{c+b_1+d+b_2} f_1(x,z,\xi)d\xi,$$

$$\sigma_{lz} = \frac{2q_1}{\pi}\int_{c}^{c+b_1} f_2(x,z,\xi)d\xi + \frac{2q_2}{\pi}\int_{c+b_1+d}^{c+b_1+d+b_2} f_2(x,z,\xi)d\xi,$$

and the corresponding graphs of displacements and stresses in Fig. 5, 6, 7.

The study of the dependence of stresses in solid and liquid phases on the distance between the objects showed that with the separation of objects from each other, normal stresses in the solid phase found by the kinematic model fade out 40 % faster than similar stresses found by the Flaman solution.

Basing on the expansion of the fundamental solution for the two-phase half-space, we considered several problems: about the action of the load distributed over rectangular and circular platforms, and about the action of the load from the interaction of two objects (spatial case). We completed the calculation of the stress and strain state for all cases. z = 2 m, d = 2 m, d = 4 m, d = 6 m.

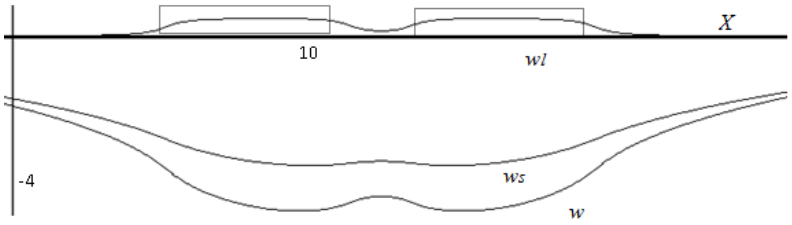

Figure 5. Vertical displacements of points in the section z = 0.5 m, $w_s w_l$ is according to the kinematic model, w – by the Flaman solution.

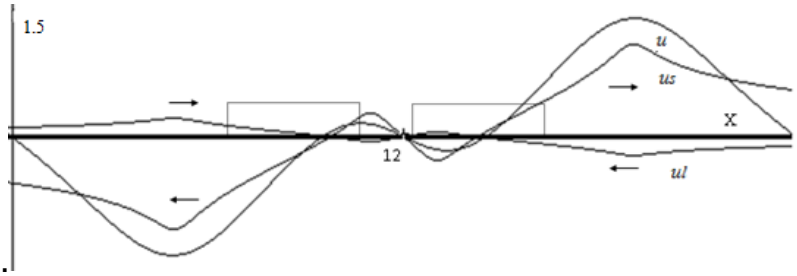

Figure 6. Horizontal displacements of points in the section z = 0.5 m.

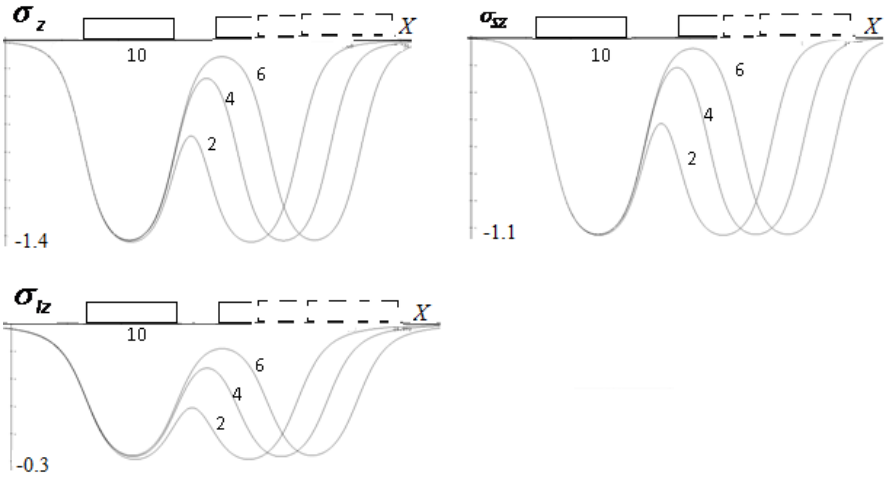

Figure 7. Dependence of stresses in the cross section z = 2 m on the distance between the objects d = 2 m, d = 4 m, d = 6 m.

The problem of the action of a concentrated force F on an elastic two-phase half-space is considered above. Here are the graphs of normal stresses in fractions of force F in different sections (Fig. 8):

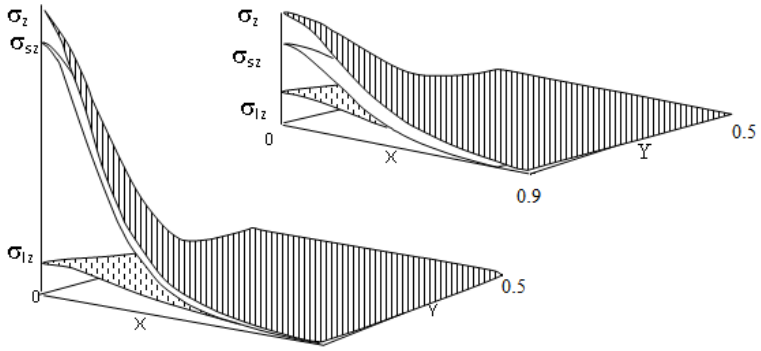

Figure 8. Change in vertical stresses in solid σ_{sz}, liquid σ_{lz} phases and the total ones σ_z in sections z = 1, z = 5.

Fig. 9 shows the graphs of displacements from the action of a load distributed over a rectangle with a parameter a^2 = 0.1(1/m) and different values of the coordinate Z.

$$u_S = \frac{F(1+\nu)}{2\pi E_S} \int_{-b}^{b} \int_{-l}^{l} \left(\frac{1}{R^2} - a^2 e^{-a^2 R} \int_{\rho}^{R} \frac{e^{a^2 R}}{R^2} dR \right) \left(\frac{zr}{R} - \frac{(1-2\nu)Rr}{R+z} \right) d\xi d\eta .$$

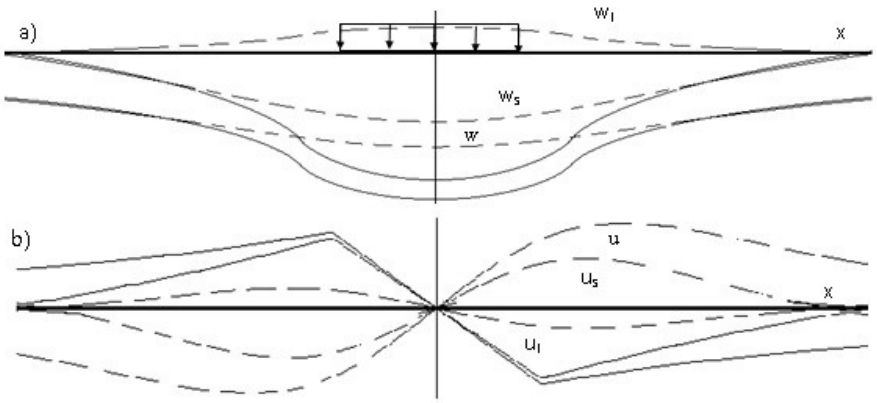

Figure 9. Graphs a) vertical and b) horizontal movements along the X axis for z = 0 (—)and z = 2 (---)by the Boussinesq solution (u,w) and by the kinematic model.

It follows from the graphs that the vertical displacements of the skeleton due to the unloading contribution of the liquid phase on the axis of symmetry for z = 2 decreased by 30 %. The maximum values of the horizontal movements of the skeleton decreased by 40 %.

The vertical stresses in the solid phase decrease faster than the total ones, therefore, the vertical displacements of the skeleton particles decrease faster than the vertical displacements obtained by the Boussinesq solution. Consequently, taking account of the liquid phase leads to the fact that the two-phase base becomes more rigid compared to the single-phase base. Fig. 11 shows graphs of pore pressures which vary over time.

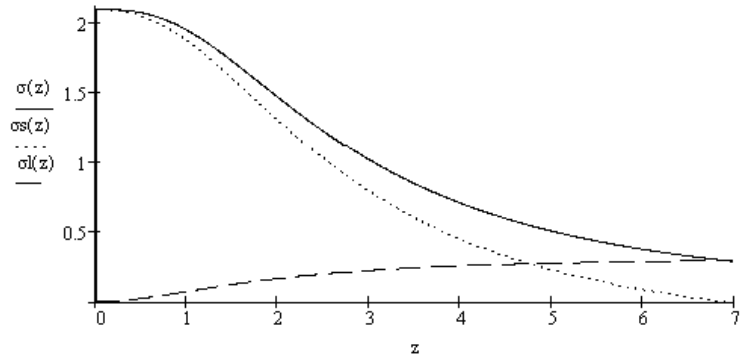

Figure 10. Distribution of stresses in depth at points under the center of the circle: total – σ, in solid σ_s and liquid σ_l phases.

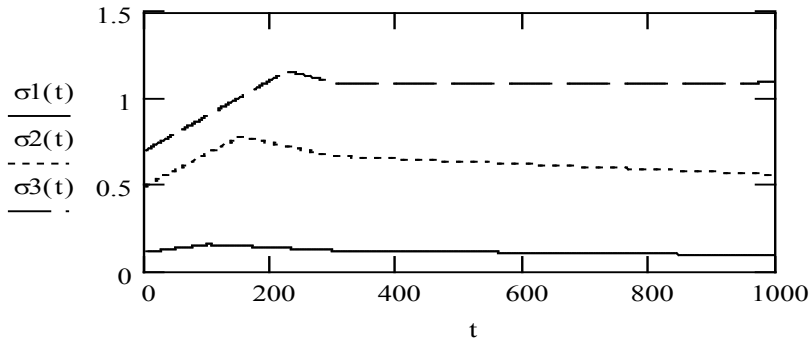

Figure 11. Change in time of pore pressure at points: x = 0, z_1 = 1/5$b_{(—)}$, z_2 = $b_{(\cdots)}$, z_3 = 5$b_{(- - -)}$.

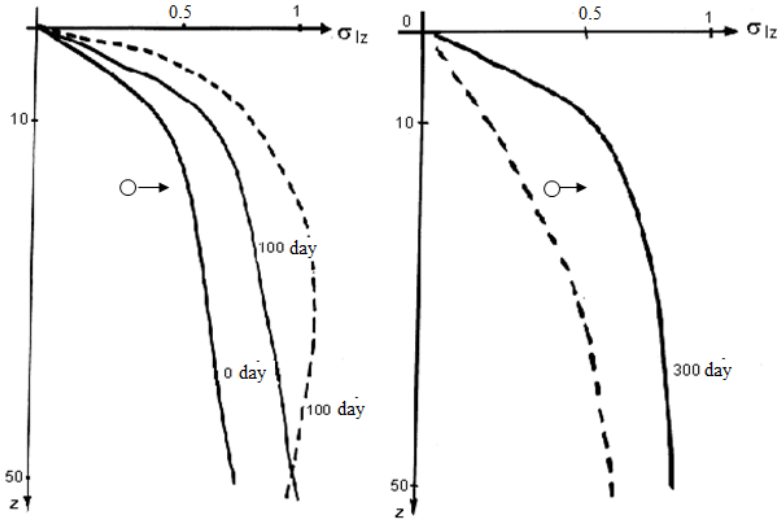

Figure 12. Comparison of the research results of pore pressure according to two models: (- - -) – according to the theory of filtration consolidation; (_____) – according to the kinematic model.

For all fixed spatial points, the pore pressure varies nonmonotonically over time. The non-uniformity of the change in pore pressure at a constant load over time reflects the peculiarity of a two-phase system. The process of pressure redistribution between phases is nonmonotonic. The maximum value of pore pressure lags in time with increasing depth, i.e. for $z = 1/5b$ the maximum value of pore pressure is reached at time

t = 100 days, and for $z = 5b$ the maximum is reached after 200 days**.** This effect was first established by L.S. Amaryan in experiments with monolithic large-sized samples.

Let us compare the obtained solution with the well-known theoretical result of V.G. Korotkin given in the monograph [22]. In the problem we investigate the distribution of pore pressure in depth during the filtration consolidation of the base from the action of a uniformly distributed load. The soil characteristics are given: a = 0.01 cm²/kg, $\varepsilon_0 = 1$, κ = 1.16·10^{-6} cm·s, the width of the strip foundation is b = 10 m. The book contains graphs of pore pressure for time T = 100, 300, 1000 и 10000 days, plotted in shares $p \cdot b/q$. The comparison was carried out only for T = 100 и 300 days, because for T = 1000 days the consolidation process almost ends and the pore pressure differs little from zero. For T = 10000 according to the theory of filtration consolidation, the pore pressure vanishes (Fig. 12).

4. Conclusion

1. The reliability of the model under consideration is shown by comparing the theoretical pore pressures with the data of a laboratory experiment LS Amaryan conducted on a sample of water-saturated peat [18]. The greatest discrepancy of 18 % is observed at the points of maximum pore pressure function. For the asymptotic value of the pore pressure function (i.e., residual pore pressure), the discrepancy between the calculated and experimental data is not more than 5 %. Comparison with the results of a full-scale experiment F.F. Zekhnieva the maximum discrepancy at the points of maximum pore pressure was 23 % and the discrepancy in residual pore pressures was 7 %.

2. In problems of the Flaman type and Boussinesq type, the stress and strain state analytically accurately decomposes into two phases (soil skeleton + pore water). From a comparison of surface sediment for single-phase and two-phase bodies, it follows that the influence of pore water on the soil skeleton manifests itself in their rapid decrease to 40 %.

3. The solution of problems in a viscoelastic formulation by the broken line method allowed us to describe the consolidation process over time and compare the result with the well-known solution obtained by the theory of filtration consolidation. For all fixed spatial points, the pore pressure varies nonmonotonically with time, and the initial value is less than the final value corresponding to a stabilized state. The non-uniformity of the change in pore pressure at a constant load over time reflects the experimentally defined feature of a two-phase system. In all solutions, we numerically analyzed and graphically presented the reduction of stresses and displacements in the skeleton due to the unloading effect of pore water. Pore pressures can reach up to 70 % of the total stresses.

4. New analytical formulas are obtained for stresses and displacements in the soil skeleton and pore water when loaded with typical loads. The solutions, in contrast to single-phase soil, take into account the influence of pore water, that is, they determine the deformed condition of the base from two-phase viscoelastic soil. The calculation formulas for the final sediments corresponding to the stabilized state of the base, without a description of the consolidation process, are recommended to be used at the design stage of buildings. This will allow taking into account the influence of pore water on the soil skeleton and providing for measures to improve the safety of their construction and operation.

References

1. Nguyen, P.D. The dependence of the strength properties of soil on its physical state. Magazine of Civil Engineering. 2012. 35(9). Pp. 23–28. DOI: 10.5862/MCE.35.3
2. Liu, E.L., Lai, Y.M., Wong, H., Feng, J.L. An elastoplastic model for saturated freezing soils based on thermo-poromechanics. International Journal of Plasticity. 2018. 107. Pp. 246–285. DOI: 10.1016/j.ijplas.2018.04.007
3. Abelev, M.Yu. Features of the construction of structures on soft water-saturated soils. Industrial and Civil Engineering. 2010. 3. Pp. 12–13.
4. Oyegbile, B., Oyegbile, B.A. Applications of geosynthetic membranes in soil stabilization and coastal defense structures. International Journal of Sustainable Built Environment. 2017. 6(2). Pp. 636–662. DOI: 10.1016/j.ijsbe.2017.04.001
5. Usmanov, R., Mrdak, I., Vatin, N., Murgu, I.V. Reinforced soil beds on weak soils. Applied Mechanics and Materials. 2014. 633–634. Pp. 932–935. DOI: 10.4028/www.scientific.net/AMM.633-634.932
6. Mirsaidov, M.M., Sultanov, T.Z. Use of linear heredity theory of viscoelasticity for dynamic analysis of earthen structures. Soil Mechanics and Foundation Engineering. 2013. 49(6). Pp. 250–256. DOI:10.1007/s11204-013-9198-8
7. Sultanov, T.Z., Khodzhaev, D.A., Mirsaidov, M.M. The assessment of dynamic behavior of heterogeneous systems taking into account non-linear viscoelastic properties of soil. Magazine of Civil Engineering. 2014. 45(1). DOI: 10.5862/MCE.45.9
8. Mirsaidov, M.M., Sultanov, T.Z. Assessment of stress-strain state of earth dams with allowance for non-linear strain of material and large strains. Magazine of Civil Engineering. 2014. 49(5). Pp. 73–82+136–137. DOI: 10.5862/MCE.49.8
9. Khudayarov, B.A., Turaev, F.Z. Nonlinear vibrations of fluid transporting pipelines on a viscoelastic foundation. Magazine of Civil Engineering. 2019. 86(2). Pp. 30–45. DOI: 10.18720/MCE.86.4

10. Maltseva, T., Saltanova, T., Chernykh, A. Modelling a Reinforced Sandy Pile Rheology when Reacting with Water-saturated Ground. Procedia Engineering. 2016. 165. Pp. 839–844. DOI: 10.1016/j.proeng.2016.11.782
11. Maltseva, T., Saltanova, T. Modelling of Water-Saturated Grounds under a Curved Section of an Oil and Gas Pipeline. MATEC Web of Conferences. 2016. 73. DOI: 10.1051/matecconf/20167301022
12. Zhi Yong Ai, Ye Cheng Dai, Yi Chong Cheng. Time-dependent analysis of axially loaded piles in transversely isotropic saturatedviscoelasticsoils. Engineering Analysis with Boundary Elements. 2019. 101. Pp. 173–187. DOI: 10.1016/j.enganabound.2019.01.004
13. Sinyakov, L., Garmanov, G., Melentev, A. Strengthening and Stabilization of the Weak Water Saturated Soils Using Stone Columns. MATEC Web of Conferences. 2016. 73. DOI: 10.1051/matecconf/20167301003
14. 14. Maltseva, T., Nabokov, A., Chernykh, A. Reinforced Sandy Piles for Low-Rise Buildings. Procedia Engineering. 2015. 117. DOI: 10.1016/j.proeng.2015.08.08.15
15. Buhartsev, V.N., Nguyen Tkhay Khoang. Estimation of the soil body stability. Magazine of Civil Engineering. 2012. 35(9). Pp. 41–48. DOI: 10.5862/MCE.35.6
16. Smolin, Yu.P., Vostrikov, K.V. Compaction of saturated soils with regard to compressible pore fluid and soil creep. Bulletin of Tomsk State University of Architecture and Civil Engineering. Journal of Construction and Architecture. 2019. 21(5). Pp. 192–199. DOI: 10.31675/1607-1859-2019-21-5-192-199
17. Guan-lin, Y., Bin, Y. Investigation of the overconsolidation and structural behavior of Shanghai clays by element testing and constitutive modeling. Shanghai, China, Tongji University. 2016. 1(1). Pp. 62–77. DOI: 10.1016/j.undsp.2016.08.001
18. Maltseva, T. Mathematical modeling of water-saturated soil basements. Advances in Intelligent Systems and Computing. 2020. 982. Pp. 872–884. DOI:10.1007/978-3-030-19756-8_84
19. Bugrov, A.K., Golli, A.V., Kagan, A.A. et al. Field studies of the stress-strain state and consolidation of beds of the system of flood-protection structures in Saint-Petersburg. Soil Mech Found Eng. 1997. 34. Pp. 1–8. DOI: 10.1007/BF02465082
20. Vorontsov, V.V., Nabokov, A.V., Ovchinnikov, V.P., Tverdokhleb, S.A. The results of compression of weak water-saturated clay macro-samples through using a “soil castle”. Scientific and Technical Bulletin of the Volga Region. 2015. 1. Pp. 60–65.
21. Maltsev, L.E., Bai, V.F., Maltseva, T.V. Kinematic model of soil and biomaterials, 2002. 336 p.
22. Tsytovich, N.A., Zaretsky, Yu.K., Malyshev, M.V. et al. The forecast rate of subsidence of structures foundations. Stroyizdat, 1967. 238 p.

Contacts:

Tatyana Maltseva, maltv@utmn.ru

Elena Trefilina, e3filina@mail.ru

Tatyana Saltanova, tsaltanova@mail.ru